Filtering the Magnetohydrodynamic Effect from 12-lead ECG Signals using Independent Component Analysis

Johannes W Krug[1], Georg H Rose[1], Daniel Stucht[2], Gari D Clifford[3], Julien Oster[3]

[1] Chair for Healthcare Telematics and Medical Engineering, University of Magdeburg, Germany
[2] Department of Biomedical Magnetic Resonance, University of Magdeburg, Germany
[3] Department of Engineering Science, University of Oxford, Oxford, UK

Abstract

When recording an electrocardiogram (ECG) under the presence of the static magnetic field of a magnetic resonance (MR) scanner, the ECG signal is disturbing by the magnetohydrodynamic (MHD) effect. Due to the MHD effect, the diagnostic information contained in the ECG signal is not accessible.

This article copes with this problem by applying different Independent Component Analysis (ICA) algorithms to ECG signals corrupted by a simulated and real MHD effect.

The applied ICA methods lead to significant errors in the resulting, filtered ECGs. Especially for the ECG signals with real MHD effect, a separation of the ECG and MHD components was not possible.

1. Introduction

Besides its usage in clinical diagnostics, Magnetic Resonance Imaging (MRI) is increasingly used for minimal invasive interventions. For MR guided applications like electrophysiological studies and catheter ablations, the availability of a diagnostic electrocardiogram (ECG) could improve diagnostics and increase patient safety.

Due to the hostile MRI environment with its time-varying radio-frequency and switched gradient magnetic fields and the static magnetic field, it is not possible to record a fully diagnostic ECG inside the MR scanner. The most disturbing artefact which is caused by the MR scanner's static magnetic field is the magnetohydrodynamic (MHD) effect. The MHD effect leads to an artefact signal which mainly superimposes the ST segment and the T wave. Simulation studies of the MHD effect give an estimate on how the ECG is affected by the MHD effect [1,2]. Independent Component Analysis (ICA) was previously successfully applied to filter simulated MHD signals from the ECG [3].

In this work, different ICA algorithms are applied to ECG signals containing simulated and real MHD signals in order to eliminate the MHD components and to obtain an MHD-free ECG signal. The accuracy of clinically relevant parameters such as elevation of the ST segment and the T wave's end are estimated.

2. Theory

2.1. Problem formulation

When the ECG is measured under the presence of the MR scanner's static magnetic field $\mathbf{B}_0$, the superposition of two signal sources, namely the ECG signal and the MHD signal, is measured:

$$ECG_{MR} = ECG + MHD \tag{1}$$

The ECG and the MHD signals have their origin in two physically different sources with the ECG representing the electrical activity of the myocardium. The source for the MHD effect is the blood flow under the presence of the static magnetic field which results in the induction of a Hall voltage [1,4]. Since the blood flow velocity is highest during the cardiac output phase, the MHD effect mainly affects the ST segment and the T wave [5]. The ECG and the MHD signals overlap in time and frequency and are highly correlated.

2.2. Independent component analysis

ICA is a statistical technique and is applied to multidimensional data in order to estimate the underlying signal components. It assumes that a set of observed variables $\mathbf{x}$ originates from a stationary linear mixing process of a set of statistically independent, non-gaussian source signals $\mathbf{s}$. ICA algorithms search for a set of base functions with non-Gaussian distribution. It was shown that the ECG signal exhibits a non-Gaussian distribution [6]. The observed signals $\mathbf{x}$ and the source signals $\mathbf{s}$ are related by the so-called mixing matrix $\mathbf{A}$:

$$\mathbf{x} = \mathbf{A}\mathbf{s} \tag{2}$$

To separate all source signals, the number of observations has to be equal or larger than the number of sources. The aim of the ICA is to find the mixing matrix $\mathbf{A}$ and the demixing matrix $\mathbf{W}$ so that:

$$\widehat{\mathbf{s}} = \mathbf{W}\mathbf{x} \tag{3}$$

where $\widehat{\mathbf{s}}$ are the estimated source signals. Several algorithms have been proposed to solve this problem. Here, the FastICA [7] and the JADE algorithm [8], which have been successfully applied to ECG signals before[9], are used.

For the given application, the vector $\mathbf{x}$ contains the measured ECG signals with either simulated ($\mathbf{x}_{\mathrm{D1}}$) or real ($\mathbf{x}_{\mathrm{D2}}$) MHD effect. The estimated source signals $\widehat{\mathbf{s}}$ are analysed and those signals $\widehat{\mathbf{s}}$ which contain the MHD effect are eliminated resulting in a filtered source vector $\widehat{\mathbf{s}}_{\mathrm{filt}}$. The filtered measurement signals $\widehat{\mathbf{x}}_{\mathrm{filt}}$ are then given as:

$$\widehat{\mathbf{x}}_{\mathrm{filt}} = \mathbf{A}\widehat{\mathbf{s}}_{\mathrm{filt}} \tag{4}$$

3. Material and methods

3.1. ECG and blood flow data acquisition

The ECG signals were recorded on one healthy male volunteer aged 28 in a 3 T MR scanner (Magnetom Verio, Siemens) using a standard 12-lead Holter ECG (*CardioMem CM3000-12, GETEMED*) with a sampling rate of 1024 Hz, a resolution of 12 Bit and an analogue bandwidth rangin from 0.05 Hz to 100 Hz.

Aortic blood flow was measured using a phase contrast MRI sequence which is based on a triggered and RF spoiled gradient echo sequence [10] with TR=61.2 ms, TE=2.6 ms and a flip angle of 7°. The measurement has a temporal resolution of 61.2 ms covering a total measurement period of 887.4 ms in 15 timeframes. Post-processing of the data included noise masking, anti-aliasing and eddy current correction [11]. Flow calculations were performed using the software described in [12].Figure 1 shows the

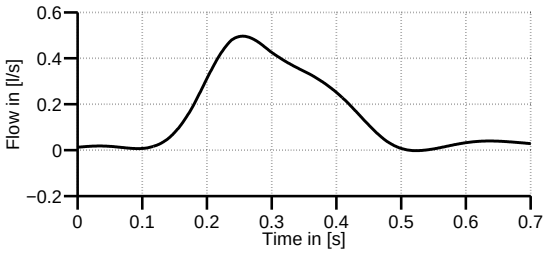

Figure 1. Estimated cardiac output closely behind the aortic valve using a 4D phase contrast MRI sequence.

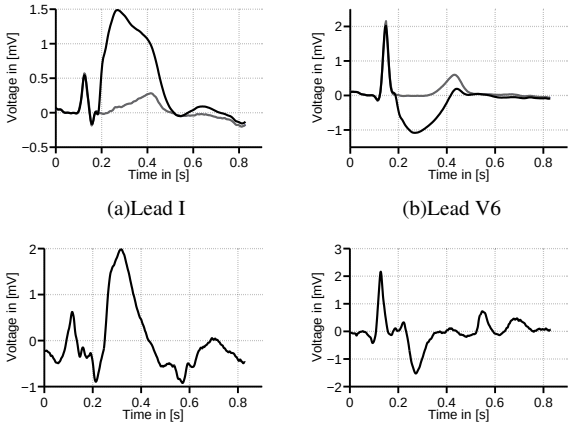

(a)Lead I (b)Lead V6

(c)Lead I (d)Lead V6

Figure 2. (a), (b): ECGs recorded outside the MR scanner (grey) and superposition with the simulated MHD signal (black). (c), (d): ECGs recorded inside the MR scanner.

volumetric blood flow rate in the aorta during one cardiac cycle. The given blood flow rate is etimated by averaging the blood flow through a cross sectional slice of the aorta closely behind the aortic valve. The estimated flow signal is used for the simulation of the MHD effect explained in Section 3.2.

3.2. ECGs with simulated MHD effect

The ECG signals recorded outside the MR scanner and the volumetric blood flow rate signal shown in Fig. 1 were mixed using a linear and stationary mixing model proposed in [2]:

$$L_i(B) = L_i(B=0) + \alpha_i B Q \quad [mV] \tag{5}$$

where L_i is the i^{th} ECG lead, B the magnetic flux density of the MR scanner, α_i the mixing coefficient for lead i and Q the flux of blood given in $^{\mathrm{cm}^3}\!/_{\mathrm{s}}$. The proposed mixing was inspired from a bidomain simulation model [2]. The mixing coefficients used in this work were derived from the relative amplitudes of the real MHD signals of each lead observed during the ECG measurements inside the MR scanner and are given in Table 1. Examples for ECG signals with simulated MHD effect ($\mathbf{x}_{\mathrm{D1}}$) are shown in Figs. 2(a) and 2(b).

3.3. ECGs with real MHD effect

Two leads of the ECG dataset $\mathbf{x}_{\mathrm{D2}}$ recorded inside the MR scanner in a feet first position are shown in Figs. 2(c) and 2(d). Compared to the simulated signal described in 3.2 and shown in Figs. 2(a) and 2(b), the scaling of the MHD effect in $\mathbf{x}_{\mathrm{D2}}$ shows a non-linear mixing behaviour for the different ECG leads and more oscillations

Table 1. Mixing coefficients α_i in $^1/_{\text{mm}}$ for all 12 ECG leads L_1 - L_{12}.

I (L_1): $0.95{\cdot}10^{-3}$	II (L_2): $0.55{\cdot}10^{-3}$	III (L_3): $-1.4{\cdot}10^{-3}$	aVR (L_4): $-0.7{\cdot}10^{-3}$
aVL (L_5): $1{\cdot}10^{-3}$	aVF (L_6): $-1.05{\cdot}10^{-3}$	V1 (L_7): $0.5{\cdot}10^{-3}$	V2 (L_8): $0.25{\cdot}10^{-3}$
V3 (L_9): $-0.43{\cdot}10^{-3}$	V4 (L_{10}): $-0.55{\cdot}10^{-3}$	V5 (L_{11}): $-0.6{\cdot}10^{-3}$	V6 (L_{12}): $-0.75{\cdot}10^{-3}$

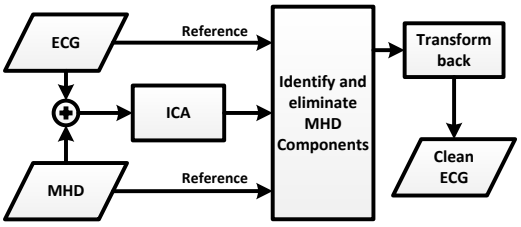

Figure 3. Mixing of ECG and MHD signal, separation of ICs containing MHD effect and back transformation.

with higher frequencies. A more detailed description of the ECG signals with real MHD effect is given in [5].

3.4. Methods

Preprocessing: Baseline wander was eliminated from the ECG signals using a cubic spline approach[1] and the DC component was removed from all leads. To increase the performance of the subsequent processing steps, the ECG signal was downsampled to 256 Hz.

Source classification: The application of the ICA algorithms to the disturbed ECG signals $\mathbf{x}$ leads to a set of base functions, namely the *independent components* (ICs) or *source signals* $\widehat{\mathbf{s}}$. The general scheme for estimating the ICs which mainly contain the ECG signal ($\widehat{s}_{\text{ECG}}$) is shown in Fig. 3. The MHD effect in $\mathbf{x}$ was attenuated by using a high-pass filter in order to apply a QRS detector[1]. The QRS detector was also applied to the estimated source signals $\widehat{\mathbf{s}}$. If the positions and numbers of QRS complexes from $\mathbf{x}$ coincide with those found in a component of $\widehat{\mathbf{s}}$, then this component was assumed to be dominated by the ECG signal. For the dataset $\mathbf{x}_{\text{D1}}$, an additional classification of the $\widehat{s}_{\text{MHD}}$ ICs was performed by correlating $\widehat{\mathbf{s}}_{\text{D1}}$ with the known MHD signal used for the simulation. This automated procedure was followed by a manual verification. All source signals $\widehat{s}_{\text{MHD}}$ and all sources $\widehat{s}_{\text{E+M}}$ containing ECG and MHD components were eliminated. The remaining sources $\widehat{\mathbf{s}}_{\text{filt}}$ consisting of either ECG signal sources $\widehat{s}_{\text{ECG}}$ or of non-identifiable sources $\widehat{s}_{\text{nID}}$ were kept to estimate the filtered measurement signal $\widehat{\mathbf{x}}_{\text{filt}}$.

[1] http://alum.mit.edu/www/gari/CODE/ECGtools/

3.5. Quality assessment

The quality of the filtered signals $\widehat{\mathbf{x}}_{\text{filt}}$ depends on the ICA's ability to separate the ECG sources $\widehat{s}_{\text{ECG}}$ from the MHD sources $\widehat{s}_{\text{MHD}}$. The quality of $\widehat{\mathbf{x}}_{\text{filt}}$ decreases if one or more ICs in $\widehat{\mathbf{s}}$ contain ECG and MHD signals ($\widehat{s}_{\text{E+M}}$) at the same time. Hence, the number of ICs identified as $\widehat{s}_{\text{ECG}}$, $\widehat{s}_{\text{MHD}}$, $\widehat{s}_{\text{E+M}}$ and $\widehat{s}_{\text{nID}}$ is given.

For the reconstructed, filtered signals $\widehat{\mathbf{x}}_{\text{filt}}$, the mean absolute differential error in the ST segment was measured against a clean reference ECG signal which was recorded outside the MR scanner. The ST segment is defined as a section of 20 ms length starting from *J point*+80 ms. The end of the T waves in $\widehat{\mathbf{x}}_{\text{filt}}$ and a clean reference ECG were annotated by a trained physician.

4. Results

4.1. Source classification

ECGs with simulated MHD effect: Both ICA algorithms identified twelve sources $\widehat{\mathbf{s}}_{\text{D1}}$. Eight sources were classified as $\widehat{s}_{\text{ECG}}$ due to the presence of QRS complexes. Two sources were classified as $\widehat{s}_{\text{MHD}}$. The remaining two sources were manually classified either as $\widehat{s}_{\text{nID}}$ or as $\widehat{s}_{\text{E+M}}$. Examples for ICs classified as $\widehat{s}_{\text{ECG}}$ and $\widehat{s}_{\text{MHD}}$ are given in Figs. 4(a) and 4(b).

ECG with real MHD effect: For the ECG signal with real MHD effect, twelve ICs $\widehat{\mathbf{s}}_{\text{D2}}$ were obtained from both ICA methods. Two sources were classified as $\widehat{s}_{\text{ECG}}$ due to a dominating QRS complex. Six sources were classified as $\widehat{s}_{\text{E+M}}$. One source was classified as $\widehat{s}_{\text{MHD}}$ due to a dominating MHD effect. Remaining ICs were classified as $\widehat{s}_{\text{nID}}$. Examples are given in Figs. 4(e) and 4(f).

4.2. Signal reconstruction and quality assessment

ECGs with simulated MHD effect: Sources classified as $\widehat{s}_{\text{MHD}}$ were removed and the remaining sources $\widehat{\mathbf{s}}_{\text{D1,filt}}$ were used to reconstruct $\widehat{\mathbf{x}}_{\text{D1,filt}}$ shown in Figs. 4(c) and 4(d). The error in the ST segment exceeds 0.1 mV in all leads. In leads II and V6, the end of the T wave could be estimated with errors below 30 ms.

ECG with real MHD effect: Examples for the reconstructed ECG signals $\widehat{\mathbf{x}}_{\text{D2,filt}}$ are shown in Fig. 4(g) and 4(h). The error in the ST segment exceeds 0.1 mV in all leads with maximum errors up to 0.8 mV. The annotation of the T wave's end was not possible.

5. Summary and conclusion

The application of ICA to ECG signals with an artificial MHD effect gave promising results in previous works

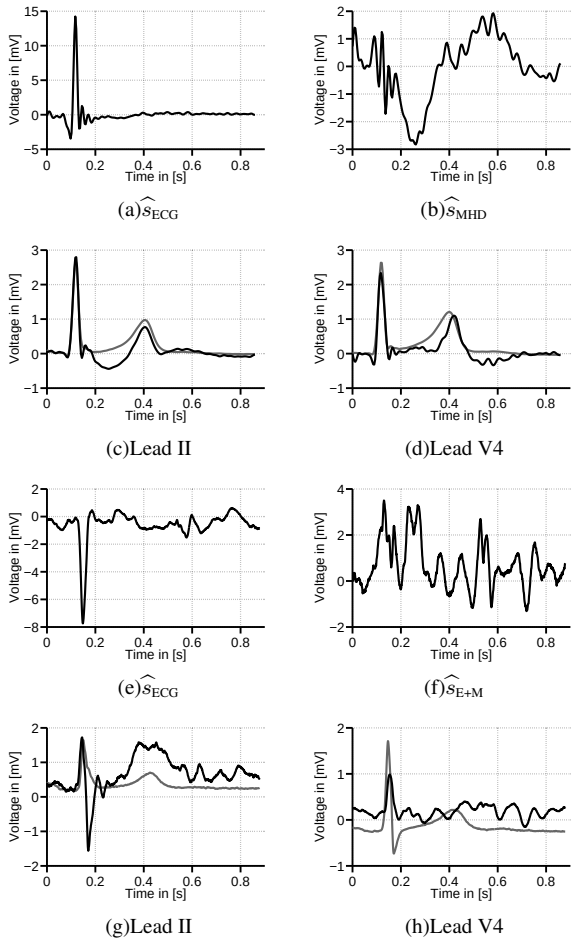

Figure 4. *Simulated dataset.* (a),(b): ICs obtained from FastICA. (c), (d): Clean ECG (gray) and $\widehat{\mathbf{x}}_{\mathrm{D1,filt}}$ (black). *Real dataset.* (e),(f): ICs obtained from FastICA. (g), (h): Clean ECG (gray) and $\widehat{\mathbf{x}}_{\mathrm{D2,filt}}$ (black).

since a linear mixing model was assumed [3]. The aim of this work was to apply ICA methods to a simulated dataset based on a linear mixing model and to ECG signals with real MHD effect.

The FastICA and JADE algorithm lead to similar results for both datasets. For the simulated dataset $\mathbf{x}_{\mathrm{D1}}$, several $\widehat{s}_{\mathrm{ECG}}$ and $\widehat{s}_{\mathrm{MHD}}$ sources were classified due to the linear mixing model. For the real dataset $\mathbf{x}_{\mathrm{D2}}$, most of the estimated sources $\widehat{\mathbf{s}}_{\mathrm{D2}}$ contain a mixture of ECG and MHD components leading to diagnostically relevant errors in the filtered signals $\widehat{\mathbf{x}}_{\mathrm{D2,filt}}$. A manual classification of the estimated source signals could not overcome this limitation.

In conclusion it can be stated that the applied ICA methods are inappropriate for separating the real MHD effect from the ECG signal since the unrealistic assumption of a linear and stationary mixing model - as applied for the simulated dataset - does not hold for the real dataset.

Acknowledgement

J Krug is funded by the Federal Ministry of Education and Research (BMBF, Germany) in context of the 'INKA' project (03IP710). J Oster is a Newton international fellow (round 2010 from the Royal Academy of Engineering). ECG recording hardware was kindly provided by GETEMED AG, Germany.

References

[1] Kinouchi Y, Yamaguchi H, Tenforde TS. Theoretical Analysis of Magnetic Field Interactions With Aortic Blood Flow. Bioelectromagnetics 1996;17(1):21–32.

[2] Martin V, Drochon A, Fokapu O, Gerbeau J, et al. Magneto-HemoDynamics in Aorta and Electrocardiograms. INRIA Rapport de recherche 2011;Version 1, 30 Sep 2011:1–38.

[3] Bhatt B, Reddy MR. ICA Based Flow Artifact Removal from ECG during MRI. In Proc Int Conf ACT 09. 2009; 241–243.

[4] Nijm G, Swiryn S, Larson A, Sahakian A. A 3D Model of Magnetohydrodynamic Voltages: Comparison with Voltages Observed on the Surface ECG during Cardiac MRI. In Proc IEEE Comput in Cardiol. 2007; 45–48.

[5] Krug J, Rose G. Magnetohydrodynamic Distortions of the ECG in Different MR Scanner Configurations. In Proc IEEE Comput in Cardiol, volume 38. 2011; 769–772.

[6] He T, Clifford G, Tarassenko L. Application of independent component analysis in removing artefacts from the electrocardiogram. Neural Comput Appl 2006;15(2):105–116.

[7] Hyvarinen A. Fast and robust fixed-point algorithms for independent component analysis. IEEE Trans Neural Netw 1999;10(3):626–634.

[8] Cardoso J, Souloumiac A. Blind beamforming for non-gaussian signals. In IEE PROC-F, volume 140. IET, 1993; 362–370.

[9] Oster J, Pietquin O, Abächerli R, Kraemer M, Felblinger J. Independent component analysis-based artefact reduction: application to the electrocardiogram for improved magnetic resonance imaging triggering. Physiological Measurement 2009;30:1381–1397.

[10] Markl M, Chan F, Alley M, Wedding K, Draney M, Elkins C, Parker D, Wicker R, Taylor C, Herfkens R, et al. Time-resolved three-dimensional phase-contrast MRI. JMRI 2003;17(4):499–506.

[11] Bock J, Kreher B, Hennig J, Markl M. Optimized preprocessing of time-resolved 2D and 3D phase contrast MRI data. In Proc. ISMRM. 2007; 3138.

[12] Stalder A, Russe M, Frydrychowicz A, Bock J, Hennig J, Markl M. Quantitative 2D and 3D phase contrast MRI: optimized analysis of blood flow and vessel wall parameters. Magnet Reson Med 2008;60(5):1218–1231.

Address for correspondence:

Johannes Krug // johannes.krug@ovgu.de
Otto-von-Guericke University of Magdeburg
Chair for Healthcare Telematics and Medical Engineering
Universitaetsplatz 2 // 39106 Magdeburg // Germany